

1 **Cu(II)/THPTA-Mediated Thiazolidine Deprotection for Living**
2 **Phages and Cell Surfaces Labeling**

3 **Chengyun Ma,¹ Guoqing Liu,¹ Jianan Sun,¹ Disheng Luo,¹ Juan Yin,² Dechun**
4 **Yang,¹ Shuo Pang,³ Wei Hou,¹ Xinya Hemu,^{*3} Bang-Ce Ye^{*1,4} and Xiaobao**
5 **Bi^{*1}**
6

7 ¹Collaborative Innovation Center of Yangtze River Delta Region Green Pharmaceuticals, College of
8 Pharmaceutical Sciences, Zhejiang University of Technology, Hangzhou, Zhejiang Province, China

9 Chengyun Ma, Guoqing Liu, Jianan Sun, Disheng Luo, Dechun Yang, Wei Hou & Xiao-Bao Bi

10 ²Zhejiang Yangshengtang Institute of Natural Medication Co., Ltd, Hangzhou, Zhejiang, China

11 Juan Yin

12 ³School of Traditional Chinese Pharmacy, China Pharmaceutical University, Nanjing, Jiangsu,
13 China

14 Shuo Pang & Xinya Hemu

15 ⁴Lab of Biosystem and Microanalysis, State Key Laboratory of Bioreactor Engineering, East China
16 University of Science & Technology, Shanghai, China.

17 Bang-Ce Ye

18 *Correspondence to: Xinya Hemu, Bang-Ce Ye & Xiao-Bao Bi (hemuxinya@cpu.edu.cn;
19 bceye@ecust.edu.cn; xbbi@zjut.edu.cn)

20 **Abstract**

21 Incorporating unnatural bioorthogonal groups into peptides and proteins offers an excellent opportunity to
22 endow them with new properties in a precise and controlled manner. Among these, the α -oxo aldehyde
23 group is particularly suitable for the post-functionalization of peptides and proteins due to its versatility
24 and stability in aqueous buffers. However, the facile and site-specific incorporation of α -oxo aldehyde
25 into proteins, especially in living systems, remains a long-lasting challenge. Here, we describe a novel
26 Cu(II)/THPTA-Mediated Thiazolidine Deprotection (CUT-METHOD) strategy for post-installation of a

27 highly-active α -oxo aldehyde moiety, which is released from a thiazolidine ring borne by a genetically
28 encoded unnatural amino acid ThzK. This reaction is performed under physiological conditions, thereby
29 enabling the chemoselective and site-specific modification of proteins via oxime ligation without
30 compromising their integrity and function. To validate its versatility, we successfully performed site-
31 specific incorporation of α -oxo aldehyde into recombinant proteins and those displayed on M13
32 filamentous bacteriophage particles and bacterial cell surfaces. In addition, by leveraging
33 Spycatcher/Spytag chemistry and oxime ligation, the bacterial cells bearing aldehyde generated via the
34 CUT-METHOD could be simultaneously decorated with two distinct functional molecules, providing a
35 novel one-pot dual labeling platform for the construction of living bacterial cell-based cancer targeting
36 systems. Put together, we have demonstrated that the CUT-METHOD strategy is a significant addition to
37 the current bioorthogonal chemistry toolbox with broad applications anticipated in the near future.

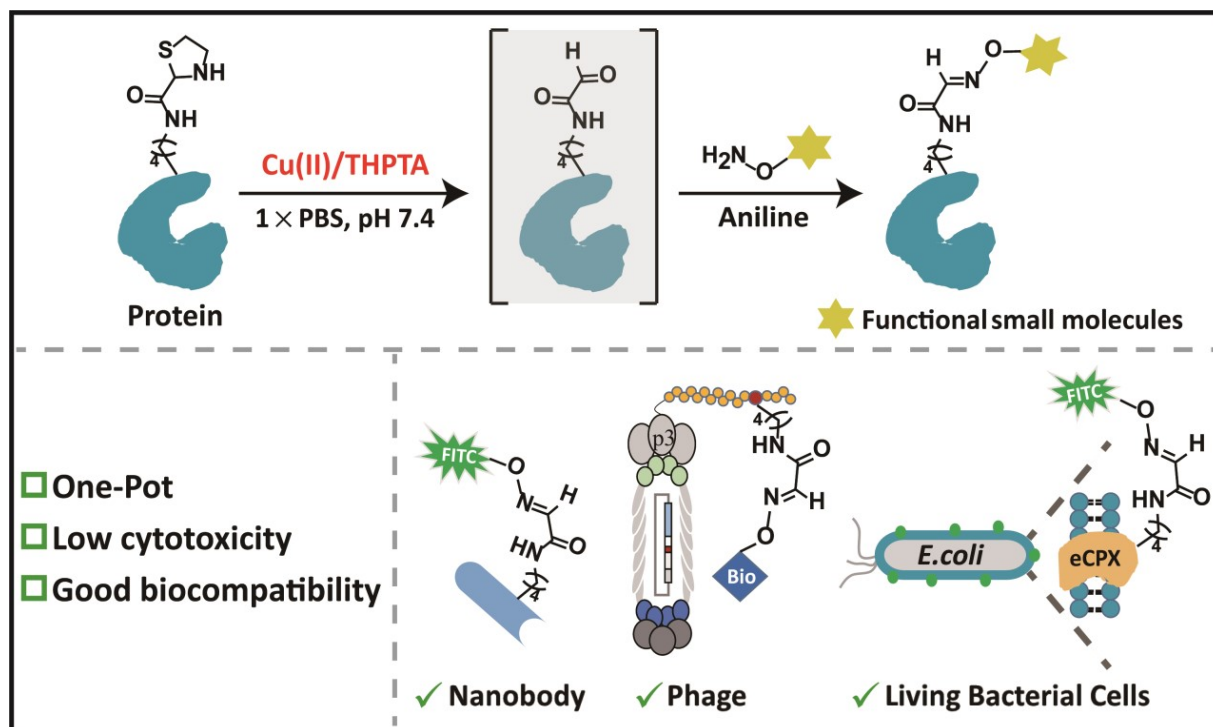
38 **Introduction**

39 Chemical modification of proteins has emerged as a pivotal technique for bestowing novel
40 functionalities upon them for diverse applications.^{1,2} However, chemoselectivity and site-specificity
41 remains a daunting task. Directly modifying the side chain functional groups of canonical amino acid
42 residues presents a straightforward approach,^{3,4} but it is often besieged by issues such as indiscriminate
43 labeling sites and the difficulty in controlling the extent of the reaction due to the presence of multiple
44 identical residues.⁵ In contrast, the incorporation of non-natural bioorthogonal groups into proteins offers
45 advantages in chemoselectivity and site-selectivity over conventional methods.⁶ Considerable efforts have
46 been made to develop chemical and biological strategies to incorporate the unique chemical handle at
47 either the two termini or internal sites of proteins.⁷⁻¹³ A notable example is genetic code expansion (GCE)
48 technology, wherein orthogonal aminoacyl-tRNA synthetase and tRNA pairs facilitate the site-specific
49 incorporation of a non-canonical amino acid equipped with a specific bioorthogonal group into a
50 predetermined location within the protein,^{14,15} thereby providing an excellent opportunity to precisely
51 modify proteins at a single-residue-resolution without affecting other residues. With the increasingly

52 expanded repertoire of genetically encodable unnatural amino acids (UAA),¹⁶ this technology has already
53 become an indispensable tool to manipulate proteins with tailor-made functionalities for diverse
54 applications, both *in vitro* and *in vivo*, such as the development of antibody-drug conjugates, the study of
55 protein post-translational modifications, and the *in situ* capture of unknown protein-protein interactions in
56 living cells.¹⁷⁻¹⁹

57 Thiazolidine chemistry serves as a pivotal "click" type of bioorthogonal reaction, wherein a
58 thiazolidine ring is formed via the specific condensation of an aldehyde and 1,2-aminothiol in aqueous
59 buffers. The exceptional chemoselectivity of this reaction has rendered it indispensable in various peptide
60 and protein chemical modification applications, including peptide cyclization, protein immobilization,
61 construction of ubiquitin dimers, and modification of living cell surfaces.²⁰⁻²³ While it has been found that
62 benzaldehydes with boronic acid substitutions can react with 1,2-aminothiols to yield stable thiazolidine
63 rings or derivatives under physiological conditions,²⁴⁻²⁷ this chemistry is generally considered a reversible
64 process.²⁸ The deprotection of the thiazolidine ring can be triggered by various stimuli, both *in vitro* and
65 *in vivo*, such as basic pH, small molecules, and transition metals.²⁹⁻³⁴ This property has made the
66 thiazolidine ring useful for temporarily caging the activity of aminothiol or aldehyde functionalities, with
67 many applications such as the deprotection of caged-Cys for native chemical ligation, traceless release of
68 cytotoxic aldehyde-containing drugs from antibodies *in vivo*, and control of the ubiquitin aldehyde probe
69 for profiling deubiquitinase in living cells.^{31,35,36,37-39} Inspired by these studies, herein a novel
70 Cu(II)/THPTA-Mediated Thiazolidine Deprotection (CUT-METHOD) strategy was successfully
71 developed. This method facilitates the release of highly active α -oxo aldehyde from the thiazolidine ring
72 of the genetically encoded thiazolidine-lysine (ThzK) in proteins under physiological conditions.
73 Consequently, it enables chemoselective and site-specific protein modification via oxime ligation without
74 compromising protein integrity and function. Furthermore, using the CUT-METHOD, for the first time
75 this chemical moiety was incorporated site-specifically into peptides displayed on phages and bacterial

76 cell surfaces without compromising their viability (Scheme 1). This study significantly broadens the
77 toolkit for precise protein engineering and cellular manipulation.



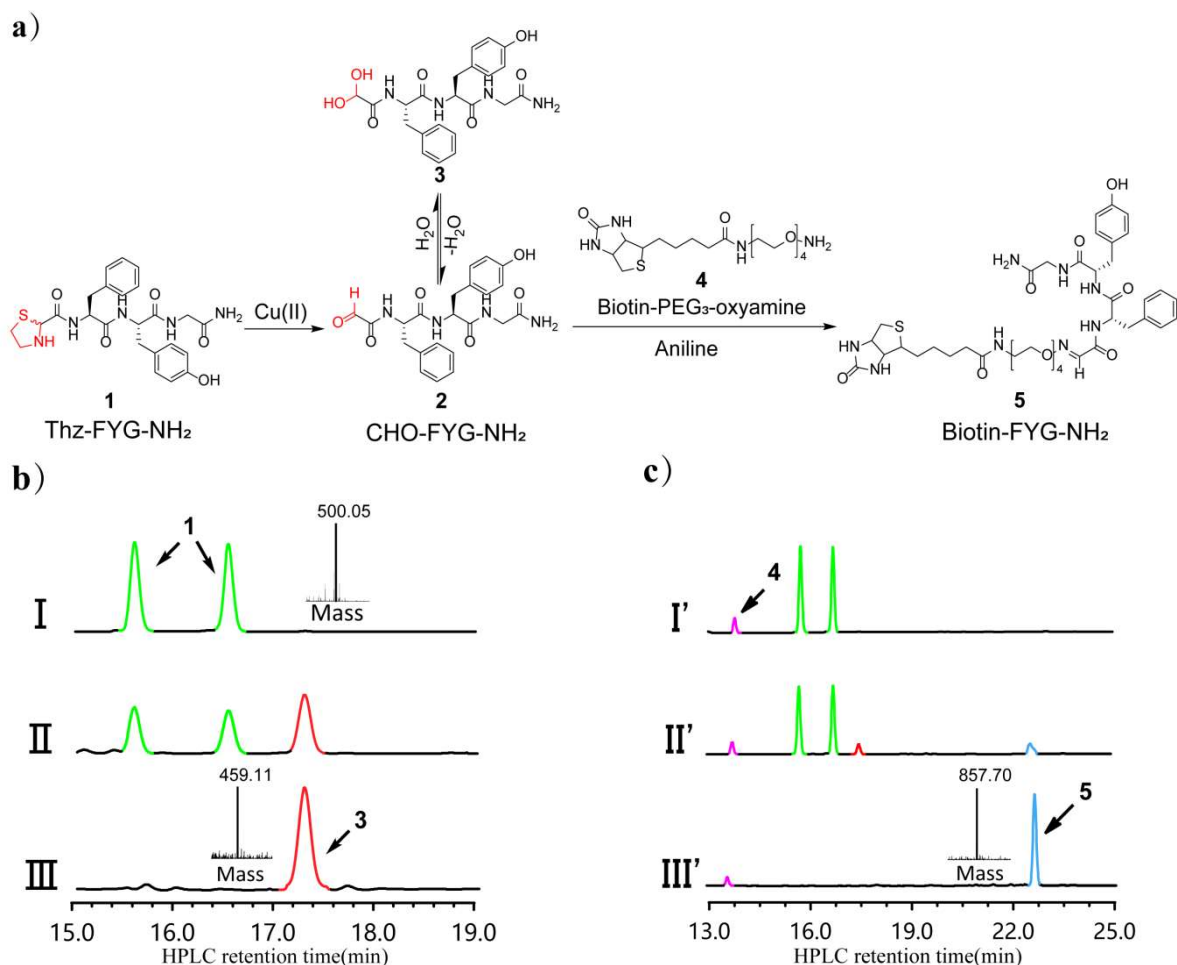
79 **Scheme 1.** Schematic presentation of the incorporation of α -oxo aldehyde into proteins, phage particles, and live
80 bacterial cell surfaces achieved by the biocompatible Cu(II)/THPTA-mediated thiazolidine deprotection. The
81 liberation of the aldehyde and its chemoselective conjugation with hydroxylamine functional reagents could be
82 carried out in a one-pot manner, with applications in nanobody, phage and bacteria cell surface chemical
83 modifications.

84 Results

85 Proof of concept study on small model peptide

86 To validate our hypothesis on Cu(II)-induced decaging of thiazolidine, we firstly demonstrate it on a
87 short model peptide Thz-FYG-NH₂ **1** due to its accessibility and ease of characterization (Figure 1a). The
88 Boc-protected thiazolidine (Thz) acid compound was synthesized conveniently following our established
89 protocols.³⁷ It was then incorporated into the N-terminus of a growing peptide on MBHA resin using
90 Fmoc chemistry via solid-phase peptide synthesis (SPPS), resulting in the expected Thz-bearing peptide **1**.

91 The purity of peptide **1** was confirmed by HPLC and MS analysis. Notably, due to the presence of mixed
92 diastereomers in the Thz compound, **1** exhibited two peaks on the HPLC profile despite having identical
93 mass values (Figure 1b, panel I). 1 mM **1** was treated with 2 mM CuSO₄ for 2 h in the reaction buffer (6
94 M guanidine, pH 6.0). HPLC analysis of the reaction mixture revealed a distinct peak, and prolonged
95 incubation for 12 h led to complete conversion of **1** into this new product. MS analysis of the new peak
96 showed a mass matching the expected hydrated form of aldehyde **3** (Figure 1b, panel II and III). To
97 further corroborate the reactivity of the released α -oxo-aldehyde group on peptide **2**, reaction was
98 performed again along with 3 mM aminooxy-biotin **4** at room temperature. HPLC analysis of the reaction
99 mixture showed the quantitative conversion of **1** into the biotinylated product **5** after 12 h, as confirmed
100 by MS analysis (Figure 1c). This data indicates that once the aldehyde was released from thiazolidine by
101 the Cu(II)-mediated ring rupture reaction, an oxime ligation with **4** happened spontaneously in a one-pot
102 manner. As 6 M guanidine is not compatible with proteins and living systems, we next attempted to
103 perform this thiazolidine deprotection reaction in PBS at neutral pH without denature reagents. However,
104 CuSO₄ exhibited poor solubility in PBS buffer at neutral and slightly basic pH, leading to the failure of
105 this test. To address this issue, we decided to test whether a water-soluble Cu(II)/THPTA complex could
106 serve as a biocompatible thiazolidine decaging reagent, considering that it has been widely used in
107 copper-catalyzed azide-alkyne cycloaddition (CuAAC) for various bioconjugation applications, including
108 protein chemical modifications and living cells labeling.⁴⁰⁻⁴² Remarkably, after 2 h treatment of **1** with
109 Cu(II)/THPTA (2 equivalents) in PBS at pH 7.4, HPLC and MS analysis revealed a complete conversion
110 of **1** into **2** (Figure S1a). Moreover, Cu(II)/THPTA mediated thiazolidine deprotection is well-compatible
111 with oxime ligation to be conducted in a one-pot manner to yield the expected biotinylated product **5** in
112 PBS at pH 7.2-7.4 (Figure S1b). Collectively, these findings indicate that Cu(II)/THPTA-mediated
113 thiazolidine deprotection (CUT-METHOD) is efficient on liberating a highly active α -oxo-aldehyde on
114 peptides by rupturing the thiazolidine ring under physiological pH. This inherent biocompatibility
115 presents great potential for the chemical modification of proteins and living cell systems.



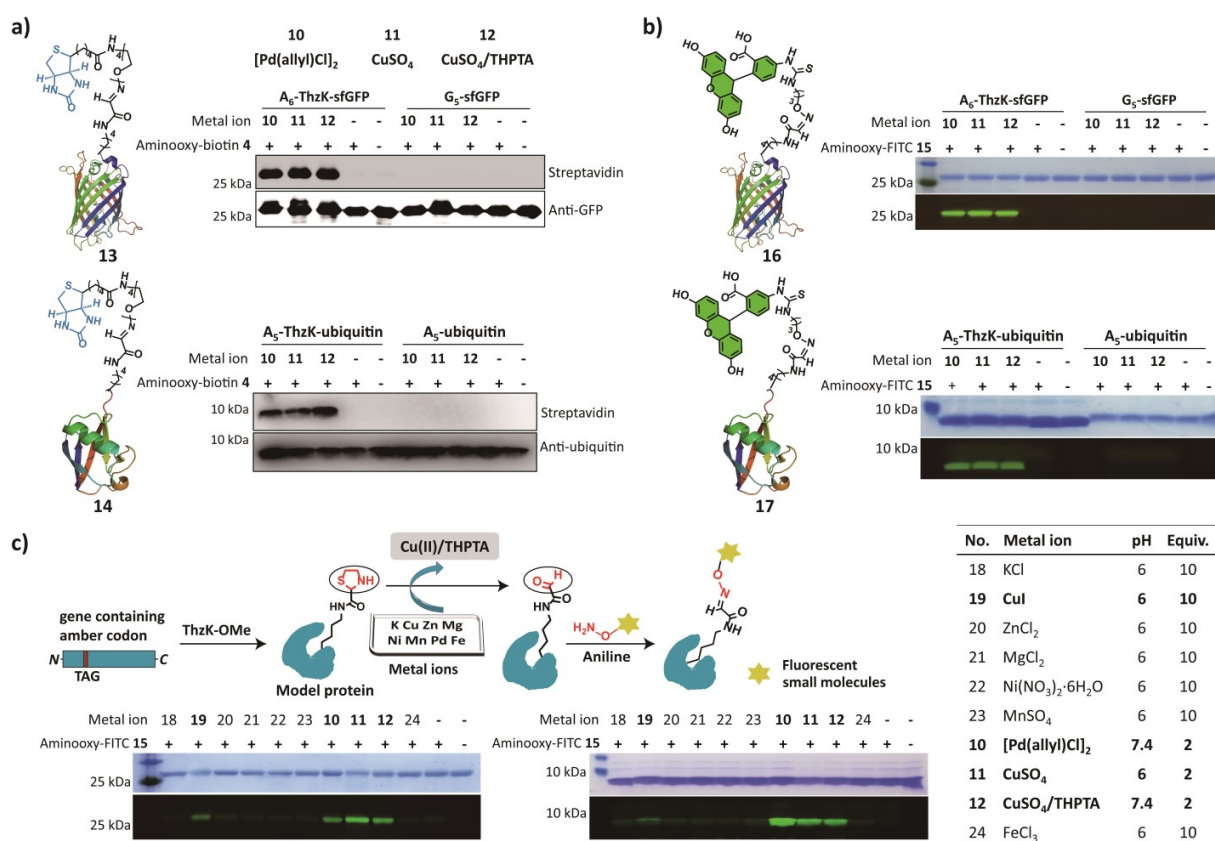
116

117 **Figure 1.** a) Scheme for the Cu(II)-mediated thiazolidine deprotection and oxime ligation for peptide modification.
 118 b) Representative C18 analytical HPLC profile and MS analysis of the starting material peptide **1** and the
 119 thiazolidine deprotection reaction treated with CuSO₄ in 6 M guanidine at pH 6.5. (I): the starting material **1** with
 120 two green peaks; the observed mass is 500.05, calcd 499.19. (II) and (III): the thiazolidine deprotection reaction for
 121 2 h and 12 h, respectively; the red peak represents the expected aldehyde **3** with an observed mass of 459.11
 122 (hydrated form), calcd 458.18; c) Representative C18 analytical HPLC profile and MS analysis of the reaction of
 123 peptide **1** with CuSO₄ and a biotin probe **4** in 6 M guanidine at pH 6.5. (I'): reaction at 0 time point, the purple peak
 124 is **4**. (II') and (III'): reaction for 1 h and 12 h, respectively; the blue peak represents the conjugated product with an
 125 observed mass of 857.70, calcd 856.99.

126 Site-specific modification of sfGFP and ubiquitin incorporating with ThzK

127 To validate the biocompatibility of CUT-METHOD, we introduced Thz functionality carried by an
 128 UAA (ThzK-OMe) into two model proteins, sfGFP and ubiquitin, using our previously established
 129 procedure.³⁷ Briefly, the pETDuet plasmid encoding sfGFP or ubiquitin with a single TAG mutation after

130 a multiple Ala sequence at the N-terminus was transformed into *E. coli* BL21(DE3) strain, along with the
131 pEVOL-MbPylRS plasmid encoding the wild type MbPylRS/tRNA pair capable of assigning ThzK-OMe
132 to the amber codon during protein translation. In the presence of 2 mM ThzK-OMe, both full-length
133 proteins were obtained with a yield of 1-2 mg/L after immobilized metal affinity chromatography (IMAC)
134 purification, yielding A₆-ThzK-sfGFP **6** and A₅-ThzK-ubiquitin **7**, respectively. In the absence of ThzK-
135 OMe, no desired proteins were harvested (Figure S2). A₆-ThzK-sfGFP **6** (30 μM) was then treated with 2
136 equivalents of Cu(II)/THPTA, and 5 equivalents of aminoxy-biotin **4** in PBS pH 7.4 at room temperature
137 for 12-18 h. In parallel, this protein was also treated with Pd(II) **10** and Cu(II) **11** for comparison. For the
138 Cu(II)-treated group, the labeling reaction was conducted in acidic PBS buffer (pH ~6) as CuSO₄ could be
139 solubilized to a moderate extent at low concentration. Meanwhile, wild type G₅-sfGFP **8** lacking ThzK
140 was treated at the same condition to serve as a negative control. Western Blot (WB) analysis revealed
141 successful biotinylation of **6** treated with Cu(II), Pd(II) and Cu(II)/THPTA **12**, whereas no bands were
142 detected in **6** in the absence of any metal ions or ThzK-installation (Figure 2a, up panel). Similarly, A₅-
143 ThzK-ubiquitin **7** and WT-A₅-ubiquitin **9** were subjected to the same treatment, also showing that only in
144 the presence of ThzK-OMe and three decaging reagents, the biotinylated band could be detected (Figure
145 2a, down panel). Besides, we found that if aminoxy-biotin **4** reaching 100 equivalents, **6** could also be
146 labeled even in the absence of the decaging reagents (Figure S3), indicating that the aminoxy group
147 itself can lead to the deprotection of thiazolidine at high concentrations and the addition of decaging
148 reagents could significantly accelerate the thiazolidine ring opening. To further demonstrate the versatility
149 of the CUT-METHOD, a fluorescent aminoxy-FITC **15** was prepared (Figure S4) and used to label the
150 aforementioned proteins under the same conditions. After the one-pot labelling reaction, fluorescent gel
151 analysis again showed that both ThzK-bearing proteins (**6** and **7**) were successfully labeled, while the
152 control protein (**8** and **9**) lacking Thz functionality and the group without metal ion treatments exhibited
153 no signal (Figure 2b). Inspired by these results, we envisaged that other transition metals may also rupture
154 the thiazolidine ring to release the aldehyde. **6** and **7** were then treated with different metal ions and **15** in
155 one-pot manner according to the conditions shown in Figure 2c, right panel. It was found that proteins



156

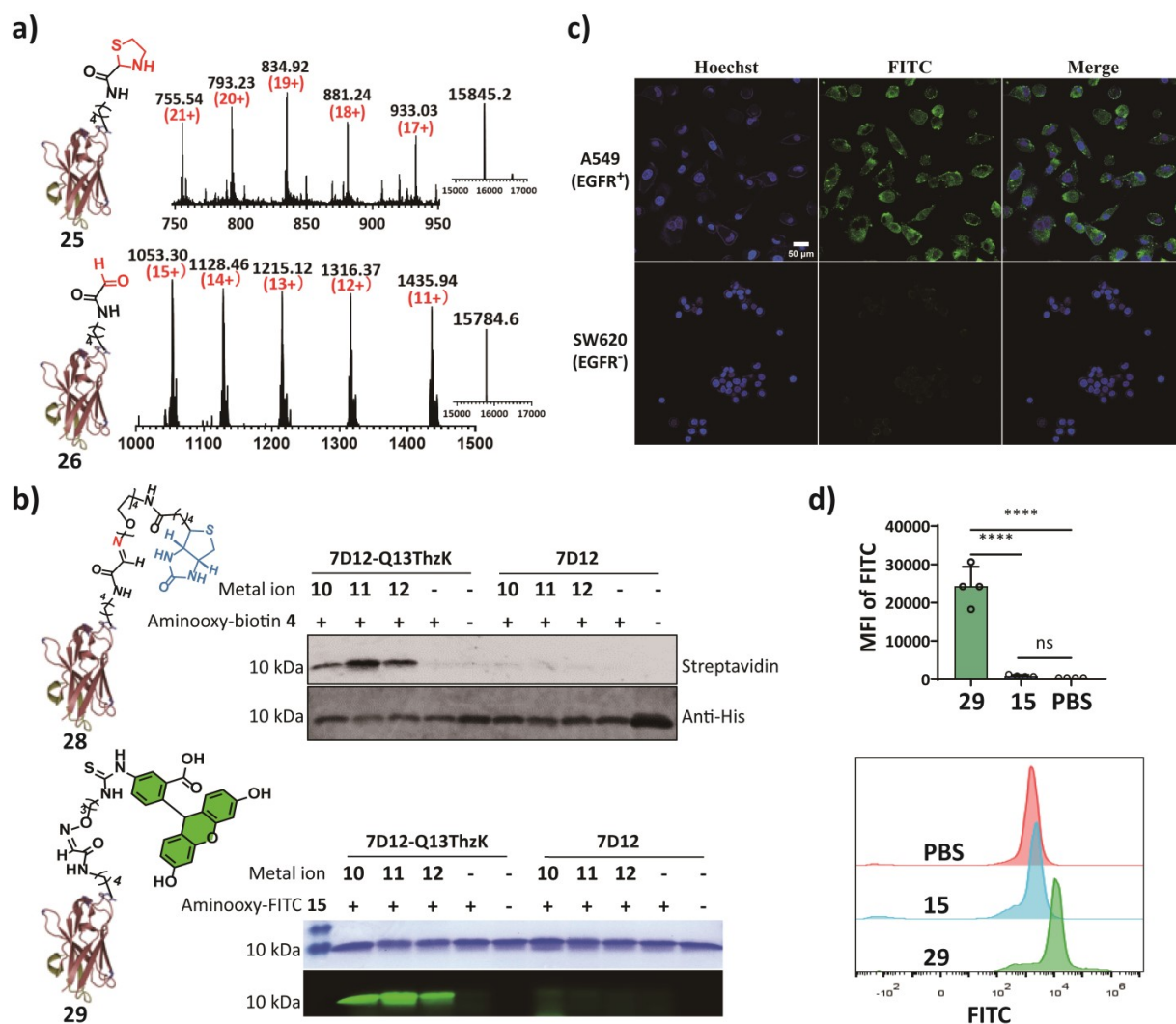
157 **Figure 2.** a) Western blot analysis of A₆-ThzK-sfGFP/WT-G₅-sfGFP (upper panel) and A₅-ThzK-Ubiquitin/WT-G₅-
 158 ubiquitin (lower panel); b) SDS-PAGE and fluorescent gel analysis of A₆-ThzK-sfGFP/WT-G₅-sfGFP (upper panel)
 159 and A₅-ThzK-Ubiquitin/WT-G₅-ubiquitin (lower panel) treated with Cu(II), Pd(II), and Cu(II)/THPTA, and labeled
 160 with FITC-ONH₂ 15 under identical conditions. Proteins were detected and visualized by Coomassie Blue staining
 161 and fluorescent emission under blue light; c) General scheme, reaction conditions, and SDS-PAGE/fluorescent gel
 162 analysis for screening metal ions capable of deprotecting the thiazolidine ring on proteins. A₆-ThzK-sfGFP/WT-G₅-
 163 sfGFP (left panel) and A₅-ThzK-Ubiquitin/WT-G₅-Ubiquitin (right panel) were labeled with FITC, and the decaging
 164 ability of individual metal ions was measured by detecting green fluorescent signals on the gel.

165 treated by treated with 10, 11, 12 and 19 were successfully labeled, as confirmed by the green fluorescent
 166 bands shown on the gel, indicating that these metal ions can mediate the thiazolidine ring deprotection to
 167 release the aldehyde. Compared to Pd(II), Cu(II), Cu(II)/THPTA, Cu(I) was less efficient based on the
 168 weaker green fluorescent signal on the gel. No such effects were observed in other metal ions (Figure 2c).
 169 These findings suggest that our CUT-METHOD is a reliable approach to release the masked aldehyde
 170 from the thiazolidine ring in intact proteins under physiological conditions using low concentrations of
 171 Cu(II)/THPTA.

172 **One-pot labeling of nanobody 7D12**

173 Nanobodies, which are single-domain antibody fragments derived from the distinctive heavy-chain
174 antibodies found in camelids, have garnered considerable attention in recent years due to their notable
175 attributes, including small size, high stability, and facile production.⁴³ As nanobodies continue to emerge
176 as potent tools for diagnostics and therapeutics, there is a growing interest in enhancing their functionality
177 through precise site-specific modifications.⁴⁴ Therefore, we aimed to test the compatibility of our CUT-
178 METHOD with nanobodies and determine whether their functions remain intact after chemical
179 transformation. The nanobody 7D12, well-known for its targeting of the Epidermal Growth Factor
180 Receptor (EGFR) on cells, was selected for this demonstration.⁴⁵ Previous studies have shown that Gln13
181 is a permissive site allowing for the encoding of UAAs without abolishing its binding capability.⁴⁶ Thus, a
182 pETDuet plasmid encoding the 7D12 nanobody harbouring a Q13TAG mutation was constructed. This
183 plasmid was then co-transformed into *E. coli* BL21(DE3) with the pEVOL-MbPylRS plasmid to produce
184 the 7D12-Q13ThzK **25** protein in the presence of 2 mM of ThzK-OMe. The expression yield reached
185 approximately 1 mg/L after IMAC purification (Figure S5). The integrity of 7D12-Q13ThzK **25** and
186 7D12-Q13CHO **26** treated by Cu(II)/THPTA was confirmed by electrospray ionization mass
187 spectrometry (ESI-MS) analysis (Figure 3a). After a 12-18 h one-pot labeling reaction, the labeled 7D12
188 was characterized by WB and fluorescent gel analysis, respectively, revealing that only in the presence of
189 Cu(II)/THPTA and ThzK-OMe could the biotinylated and fluorescent bands be detected while the WT
190 7D12 **27** lacking ThzK and 7D12-Q13ThzK without metal ions treatment exhibited no signal under the
191 same conditions (Figure 3b), which is consistent with the above results obtained with sfGFP and ubiquitin
192 labeling. To assess whether the FITC-conjugated 7D12 still retained its ability to target EGFR, two cell
193 lines, A549 (EGFR-positive) and SW620 (EGFR-negative), were tested. Remarkably, an evident green
194 rim was observed only in the A549 cell line, while no obvious signal detected in SW620, confirming the
195 preserved targeting capability and selectivity of the labeled 7D12-Q13ThzK (Figure 3c). This observation
196 was further confirmed by flow cytometry analysis (Figure 3d). These findings indicate the excellent

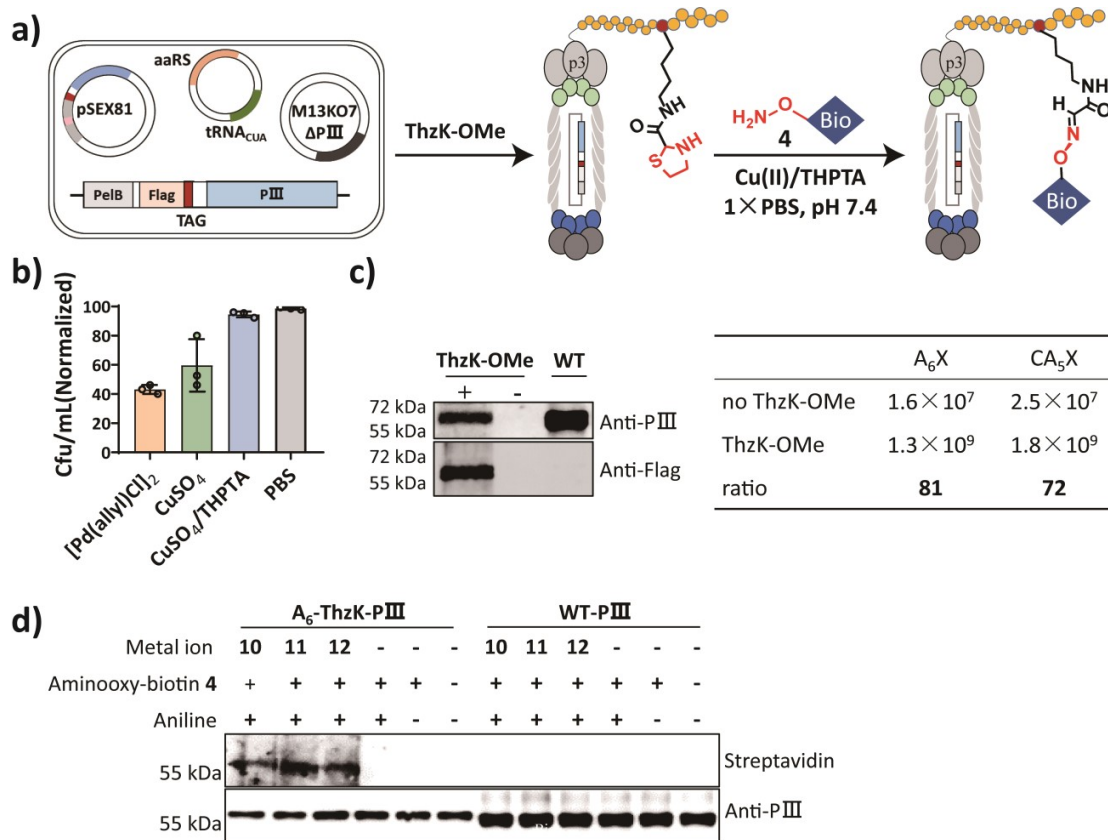
197 biocompatibility of our CUT-METHOD with intact functional proteins, highlighting its potential utility in
 198 the development of targeted protein molecules for diagnostic and therapeutic applications.



199
 200 **Figure 3.** Site-directed chemical modification of nanobody 7D12 incorporating ThzK using CUT-METHOD and
 201 oxime ligation and its characterization. a) ESI-MS analysis of 7D12-Q13ThzK **25** with the observed mass 15845.2
 202 Da, calcd 15845.4 Da (up panel) and 7D12-Q13aldehyde **26** with the observed mass 15784.6 Da, calcd 15786.3 Da
 203 (down panel); b) Western blot analysis of products generated by reacting 7D12 **25** with biotin-PEG₃-oxoamine **4**;
 204 SDS-PAGE/fluorescent gel analysis of products generated by reacting 7D12-Q13ThzK **25** with FITC-ONH₂ **15**; c)
 205 Confocal microscopy images of A549/SW620 cells incubated with 100 nM 7D12 **29** (green) for 30 min in 37°C.
 206 The nuclei were stained with Hoechst (blue). Scale bars = 50 μm; d) Mean fluorescence intensity of A549 cells
 207 incubated with 3 different samples. Statistical significance was calculated by one-way ANOVA with Tukey's
 208 multiple comparisons test (**** < 0.0001); Histogram showing fluorescence intensity distribution of A549 cells
 209 incubated with 3 different samples.

210 **Site-specific incorporation of α -oxo-Aldehyde into bacteriophage particles**

211 Phage display is a widely used technique in molecular biology and biotechnology, serving as a
212 valuable tool for exploring protein-protein interactions, protein engineering, and the discovery of
213 antibodies.^{47,48} Traditional phage display techniques can only present peptides and proteins made from the
214 20 canonical amino acids with limited chemical functionalities. To address this limitation, GCE
215 technology has been recognized as a powerful approach to enable the accurate insertion of a single or
216 even multiple UAAs into phage, expanding the chemical space of functionalities encoded by the phage
217 for various applications.⁴⁹⁻⁵³ Up to date, incorporating aldehyde moiety into phage particles has been
218 achieved by serine oxidation and pyridoxal 5'-phosphate (PLP)-mediated transformation.^{54,55} However,
219 the generated aldehyde is only confined to the N-terminus of peptide/proteins displayed on the phage.⁵⁶
220 Moreover, such chemical transformations might also inadvertently abolish other amino acids such as Cys
221 and Met, potentially compromising the phage's activity and the function of the peptides and proteins it
222 presents. A reliable technique for the site-specific incorporation of α -oxo-aldehyde into live phage
223 particles is still in need. Hence, our subsequent focus was directed to incorporate ThzK-OMe into phage
224 particles and assess the compatibility of our CUT-METHOD with live phages (Figure 4a). First, to test
225 the effects of Cu(II), Pd(II) and Cu(II)/THPTA on the viability and infectivity of phages, wild phage
226 lacking ThzK were used, as they can be very easily prepared due to rapid propagation and high yield.
227 Results show that Cu(II)/THPTA was fully compatible without any obvious adverse effects on phage
228 viability compared to PBS treatment. In contrast, long-term exposure of phages to Pd(II) would
229 significantly decrease their infectivity as shown in Figure 4b. Based on this data, we determined to use
230 Cu(II)/THPTA as the best decaging reagent due to its excellent biocompatibility. Next, to site-specifically
231 incorporate ThzK-OMe into bacteriophages, a tri-plasmids system was constructed according to previous
232 reports.^{51,57} In this system, the pSEX81 plasmid encodes either a FLAG tag-A₆X-pIII or FLAG tag-CA₅X-
233 pIII fusion protein, where 'X' denotes the incorporated ThzK. The pIII encoding sequence in the M13KO7
234 helper phage has been deleted, resulting in the inability to generate viable phage without the



235

236 **Figure 4.** a) Schematic diagram illustrating a tri-plasmid system employed to generate a phage containing ThzK at
 237 the N-terminus of pIII protein, and its labeling with biotin using CUT-METHOD and oxime ligation; b) Assessment
 238 of effect of metal ions on bacteriophage activity. Each group was repeated 3 times for titer testing and the average
 239 value was taken (retaining 3 significant figures); c). Western blot analysis depicting phage expression (FLAG-A₆X-
 240 pIII and WT) in the absence or presence of ThzK-OMe (left panel); The table presents two phage derivatives, one
 241 featuring an N-terminal CA₅X peptide and the other with a N-terminal A₆X peptide, where X denotes ThzK, along
 242 with their corresponding phage yields (CFU/mL) in the presence and absence of ThzK-OMe (left panel); d) Western
 243 blot analysis of A₆-ThzK-P_{III} and WT phage labelled with biotin-PEG₃-oxyamine 4.

244 supplementation of full-length pIII (Figure S6). Therefore, only after ThzK-OMe was successfully
 245 incorporated, could a FLAG tag-pIII fusion peptide be expressed, and intact phage particles formed with
 246 the pentavalent display of peptides-ThzK-pIII fusion protein. WB analysis shows that only in the presence
 247 of ThzK-OMe, the FLAG band could be detected using Anti-FLAG antibody, with no bands observed
 248 otherwise, indicating that ThzK-OMe have been incorporated into the phages (Figure 4c, left panel).
 249 Moreover, A₆X-phage and CA₅X-phage have a 81 and 72 fold increase in infectivity in the presence of
 250 ThzK-OMe than that of phage without ThzK-OMe supplement (Figure 4c, right panel), which is

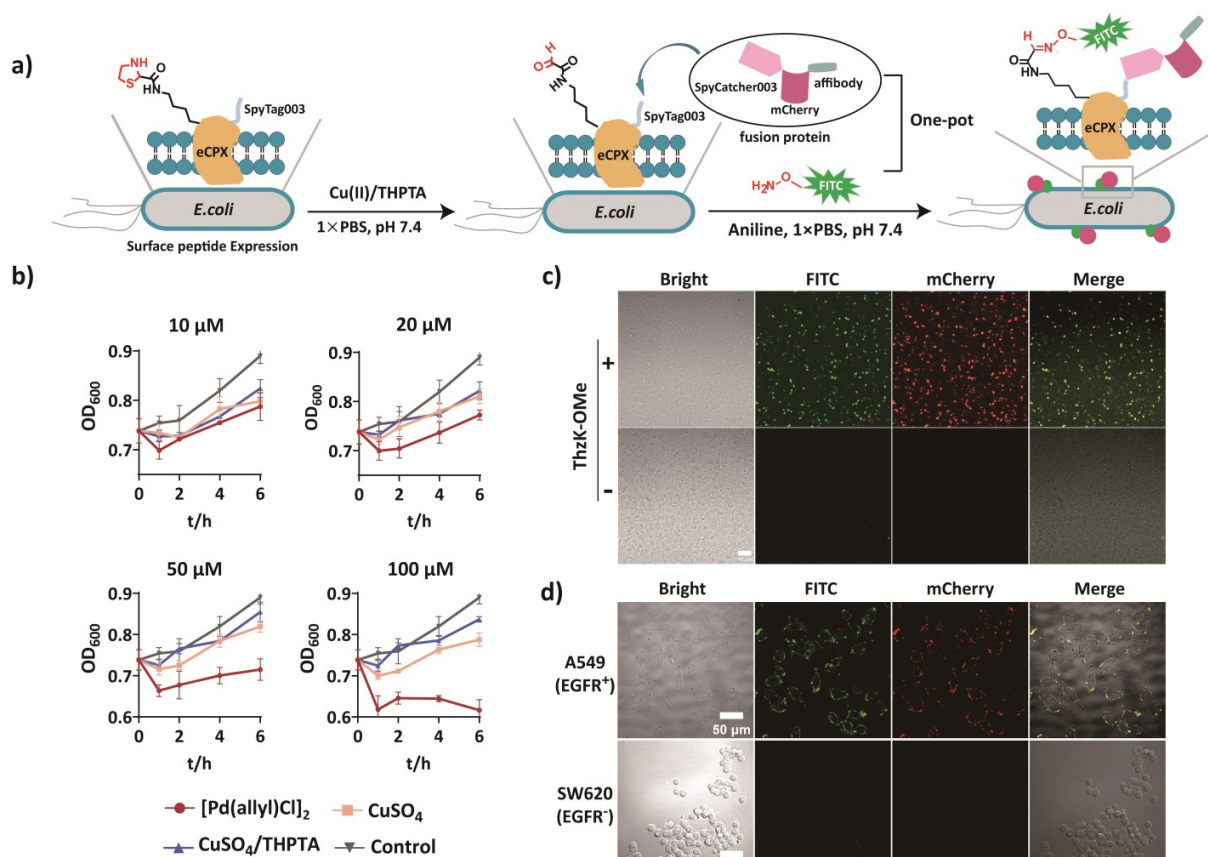
251 consistent with previous observation that phage incorporating with UAA has higher infectivity.⁵³ To
252 further verify the successful installation of ThzK-OMe on phage, ThzK-incorporating phages were treated
253 with Cu(II)/THPTA, Cu(II), Pd(II) and biotin-aminooxyl **4** at room temperature for 2 h in PBS. Wild-type
254 phages served as a negative control. WB analysis again showed that biotinylated labeled pIII was only
255 detectable in ThzK-incorporating phages, with no bands observed in the wild-type phages (Figure 4d).
256 Overall, this proof-of-concept study suggest that the combined utilization of our CUT-METHOD and
257 GCE technology enables the site-specific incorporation of α -oxo-aldehyde into phage particles, expanding
258 the chemical space of functionalities genetically encoded by the phage.

259 **One-pot dual labeling platform for bacterial surfaces decoration**

260 To further demonstrate the broad applicability of our approach, we attempted to expand it to more
261 complicated biological systems. Similar to phage display, bacterial cell surface display is also a powerful
262 biotechnology with widespread applications among others, including antibody epitope mapping and
263 bacterial cancer therapy.⁵⁸ Several chemoenzymatic strategies have been innovatively developed for
264 externally decorating bacterial cells with a variety of functional molecules.^{59,60} including those using
265 UAAs.^{61,62} Despite these advances, currently, there remains a scarcity of methods enabling one-pot,
266 bioorthogonal dual labeling of bacterial cell surfaces. To this end, we made endeavours to develop a new
267 strategy to achieve simultaneous dual labeling of bacterial cells in a one-pot fashion by combined use of
268 Spycatcher/SpyTag chemistry and our CUT-METHOD. The process involved the simultaneous
269 incorporation of ThzK and SpyTag003 (a SpyTag derivative with higher reaction kinetics in low
270 concentration)⁶³ into the peptide displayed on bacteria cell surface using eCPX system.⁶⁴ These elements
271 served as two orthogonal ligation handles for subsequent attachment of two functionalities onto cell
272 surface in a one-pot manner,⁶⁵ endowing them with fluorescent property and cancer cell-selective
273 targeting ability, as depicted in Figure 5a. As eCPX can display two different peptides at its both ends, a
274 model peptide GGGGGX followed by a FLAG tag, where X represented ThzK, and Spyttag003 were

275 introduced at the N and C terminus, respectively. This ensured that only when ThzK-OMe was
276 incorporated successfully could the full length of eCPX be detected via WB analysis using anti-FLAG
277 antibody (Figure S7). To verify whether our CUT-METHOD is compatible with living bacterial cells, we
278 first assessed the cytotoxic effects of the metal ions at different concentrations on *E. coli* over a 6 h
279 incubation period. Results demonstrated that even at the highest concentrations (100 μ M), Cu(II)/THPTA
280 exhibited minimal toxicity, contrasting with Pd(II), which resulted in the complete eradication of bacterial
281 cells at the same concentration (Figure 5b). This assay again highlights the excellent compatibility of
282 Cu(II)/THPTA with biological systems. To minimize the potential effect of metal ion treatments on
283 bacterial activity, we adopted two-step process to label cells. Firstly, bacterial cells were treated with
284 Cu(II)/THPTA for 2 h to liberate the aldehyde. Then, the Cu(II)/THPTA were removed by extensive PBS
285 washing, ensuring there is no toxic effect on their activity. To determine whether these bacterial cells
286 bearing aldehyde and SpyTag003 could be simultaneously labeled, FITC-aminooxyl 15 and mCherry-
287 SpyCatcher003 were co-incubated with cells in PBS for 4 h at 37°C. Confocal microscopy analysis
288 revealed colocalized green and red fluorescent signals, observable only in the presence of ThzK-OMe
289 (Figure 5c, upper panel), which was attributed to bacteria surface-conjugated FITC and mCherry,
290 respectively. This data suggests the successful attachment of two functional molecules concurrently via
291 oxime ligation and isopeptide bond formation. In contrast, in the absence of ThzK-OMe, no fluorescent
292 signals were detected on the bacterial cell surface (Figure 5c, down panel).

293 Bacterial cancer therapy is increasingly recognized as a promising method for cancer treatment,
294 leveraging bacteria to target and eliminate cancer cells through direct destruction or by eliciting an
295 immune response against the tumor.^{66,67} To explore the potential of our method in generating
296 fluorescently labeled bacterial cells with targeted tumor-binding ability, a trifunctional affibody-mCherry-
297 SpyCatcher003 fusion protein was designed (Figure S8), in which the affibody can target EGFR over
298 expressed on cancer cells, mCherry was used for red fluorescent detection and SpyCatcher003 mediated
299 the installation of this protein onto the bacteria cells by reacting with the surface displayed SpyTag003.



300

301 **Figure 5.** a) Schematic representation illustrating the dual labeling of live bacterial cell surfaces in a one-pot fashion
 302 using oxime ligation and SpyCatcher/SpyTag chemistry, along with their tumor cell targeting applications. ThzK
 303 and SpyTag003 were incorporated into the N- and C-terminal ends of the surface-localized eCPX on *E. coli*,
 304 respectively, and the aldehyde was released using the CUT-METHOD; b) Effects of different metal ions on the
 305 growth activity of *E. coli* at four different concentrations during a 6 h period; c) Confocal microscopy images of
 306 FITC and mCherry-labeled *E. coli*. Scale bar = 10 μm ; d) Representative confocal microscopy images of
 307 A549/SW620 cells labeled with FITC and mCherry-labeled *E. coli* samples at 37°C for 1 h. Rinse cells with PBS
 308 before observation. Scale bar = 50 μm .

309 Then, the bacterial cells underwent the same one-pot labeling procedure as previously described.
 310 Evaluation of efficacy in targeting tumors was tested using A549 and SW620 cells. Confocal microscopy
 311 analysis revealed green and red spots exclusively on the surface of A549 cells, indicating the adherence of
 312 dual-color labeled bacteria. By contrast, no signal was observed in EGFR-negative SW620 cells, which is
 313 attributed to the lack of specific interaction between affibody and EGFR (Figure 5d and S9-10).
 314 Collectively, these findings suggest that oxime ligation is bioorthogonal to Spycatcher/Spytag chemistry,
 315 and the combination of these two reactions along with our CUT-METHOD provides a reliable and

316 biocompatible approach to decorate living cells with two distinct functional molecules. This innovative
317 one-pot labeling platform holds potential for diverse applications in the future, including the development
318 of new live cell drugs for tumor therapy.

319 **Discussion**

320 In summary, In this study, we present a novel method for liberating the highly active α -oxo-aldehyde
321 from a thiazolidine ring under physiological conditions, leveraging a stable and biocompatible
322 Cu(II)/THPTA complex. Coupled with genetic code expansion and oxime ligation, this work provides a
323 robust and biocompatible tool for site-specific and chemoselective modifications of peptides, proteins,
324 phage particles, and living bacterial cells without compromising their normal functions. Despite the
325 widespread use of Cu(II)/THPTA in click chemistry,⁴¹ our study represents the first exploration of its
326 utility in generating aldehydes by rupturing the thiazolidine ring under physiological buffer systems. Its
327 excellent biocompatibility allows for seamless integration of the aldehyde into proteins and biological
328 systems. Moreover, it could be envisaged that by combined with click chemistry, this shared reagent
329 would also be also useful for synthesizing the dual-modified peptide/protein conjugates in a one-pot
330 manner. Additionally, our work presents other innovative aspects. Through genetic code expansion, we
331 achieved the site-specific incorporation of α -oxo-aldehyde into peptides displayed on phage particles,
332 expanding the chemical space of functionality that can be genetically encoded in phages. This
333 breakthrough enables precise modification of phages for potential drug delivery and opens avenues for
334 selecting novel affinity peptides carrying the aldehyde or its derivatives. We also present a novel one-pot,
335 bioorthogonal dual labeling platform by the combined use of SpyCatcher/SpyTag chemistry with oxime
336 ligation,⁶⁸ facilitating the facile and fast generation of dual-functionalized bacteria with tailor-made
337 properties for various applications. Overall, our CUT-METHOD offers a versatile approach for
338 selectively modifying biomolecules and living cells, with vast potential in chemical biology and
339 biotechnology, such as on-demand manipulation of protein activity in living cells.

340 **Supporting Information**

341 Detailed methods and experimental procedures could be found in the Supporting Information file,
342 including recombinant protein expression, phage preparation, dual-labeling of bacterial cell surface,
343 HPLC, ESI-MS, SDS-PAGE, Western blot, et al.

344 **Contributions**

345 X. B. conceived, designed and supervised the project. C. M. performed the experiments, collected and
346 analyzed data. H. X., B. Y and X. B. wrote the manuscript. J. Y. collected the confocal data of labeled
347 bacterial cells. G. L. completed the model peptide study. J. S. and D. Y. conducted some cell labeling
348 experiments. D. L. and W. H. completed the synthesis of FITC-ONH₂, and S. P. assisted in the ESI-MS
349 analysis of the protein. All authors discussed the results and commented on the manuscript.

350 **Data Availability**

351 All other relevant data that support the findings of this study are available from the corresponding authors
352 on reasonable request.

353 **References**

- 354 1. Spicer, C. D.; Davis, B. G. Selective Chemical Protein Modification. *Nat. Commun.* **2014**, *5* (1), 4740.
- 355 2. Zhang, C.; Welborn, M.; Zhu, T.; Yang, N. J.; Santos, M. S.; Van Voorhis, T.; Pentelute, B. L. II-Clamp-
356 Mediated Cysteine Conjugation. *Nat. Chem.* **2016**, *8* (2), 120–128.
- 357 3. Boutureira, O.; Bernardes, G. J. L. Advances in Chemical Protein Modification. *Chem. Rev.* **2015**, *115* (5), 2174–
358 2195.
- 359 4. Shadish, J. A.; DeForest, C. A. Site-Selective Protein Modification: From Functionalized Proteins to Functional
360 Biomaterials. *Matter.* **2020**, *2*(1), 50–77.
- 361 5. Baslé, E.; Joubert, N.; Pucheault, M. Protein Chemical Modification on Endogenous Amino Acids. *Chem. Biol.*
362 **2010**, *17* (3), 213–227.
- 363 6. Wang, Y.; Zhang, J.; Han, B.; Tan, L.; Cai, W.; Li, Y.; Su, Y.; Yu, Y.; Wang, X.; Duan, X.; Wang, H.; Shi, X.;
364 Wang, J.; Yang, X.; Liu, T. Noncanonical Amino Acids as Doubly Bio-Orthogonal Handles for One-Pot Preparation
365 of Protein Multiconjugates. *Nat. Commun.* **2023**, *14* (1), 974.

366 7. Morgan, H. E.; Turnbull, W. B.; Webb, M. E. Challenges in the Use of Sortase and Other Peptide Ligases for
367 Site-Specific Protein Modification. *Chem. Soc. Rev.* **2022**, *51* (10), 4121–4145.

368 8. Fernández-Suárez, M.; Baruah, H.; Martínez-Hernández, L.; Xie, K. T.; Baskin, J. M.; Bertozzi, C. R.; Ting, A. Y.
369 Redirecting Lipoic Acid Ligase for Cell Surface Protein Labeling with Small-Molecule Probes. *Nat. Biotechnol.*
370 **2007**, *25* (12), 1483–1487.

371 9. Rush, J. S.; Bertozzi, C. R. New Aldehyde Tag Sequences Identified by Screening Formylglycine Generating
372 Enzymes in Vitro and in Vivo. *J. Am. Chem. Soc.* **2008**, *130* (37), 12240–12241.

373 10. Nguyen, G. K. T.; Qiu, Y.; Cao, Y.; Hemu, X.; Liu, C.-F.; Tam, J. P. Butelase-Mediated Cyclization and
374 Ligation of Peptides and Proteins. *Nat. Protoc.* **2016**, *11* (10), 1977–1988.

375 11. Gilmore, J. M.; Scheck, R. A.; Esser-Kahn, A. P.; Joshi, N. S.; Francis, M. B. N-Terminal Protein Modification
376 through a Biomimetic Transamination Reaction. *Angew. Chem. Int. Ed. Engl.* **2006**, *45* (32), 5307–5311.

377 12. Zeng, Y.; Shi, W.; Liu, Z.; Xu, H.; Liu, L.; Hang, J.; Wang, Y.; Lu, M.; Zhou, W.; Huang, W.; Tang, F. C-
378 Terminal Modification and Functionalization of Proteins via a Self-Cleavage Tag Triggered by a Small Molecule.
379 *Nat. Commun.* **2023**, *14* (1), 7169.

380 13. Yi, L.; Sun, H.; Wu, Y.-W.; Triola, G.; Waldmann, H.; Goody, R. S. A Highly Efficient Strategy for
381 Modification of Proteins at the C Terminus. *Angew. Chem. Int. Ed. Engl.* **2010**, *49* (49), 9417–9421.

382 14. Wang, L.; Schultz, P. G. Expanding the Genetic Code. *Angew. Chem. Int. Ed. Engl.* **2004**, *44* (1), 34–66.
383 [D.org/10.1002/anie.200460627](https://doi.org/10.1002/anie.200460627)

384 15. Wan, W.; Tharp, J. M.; Liu, W. R. Pyrrolysyl-tRNA Synthetase: An Ordinary Enzyme but an Outstanding
385 Genetic Code Expansion Tool. *Biochim. Biophys. Acta.* **2014**, *1844* (6), 1059–1070.

386 16. Zhu, Y.; Ding, W.; Chen, Y.; Shan, Y.; Liu, C.; Fan, X.; Lin, S.; Chen, P. R. Genetically Encoded Bioorthogonal
387 Tryptophan Decaging in Living Cells. *Nat. Chem.* **2024**, *16* (4), 533–542.

388 17. Oller-Salvia, B.; Kym, G.; Chin, J. W. Rapid and Efficient Generation of Stable Antibody-Drug Conjugates via
389 an Encoded Cyclopropene and an Inverse-Electron-Demand Diels-Alder Reaction. *Angew. Chem. Int. Ed. Engl.*
390 **2018**, *57* (11), 2831–2834.

391 18. Weyh, M.; Jokisch, M.-L.; Nguyen, T.-A.; Fottner, M.; Lang, K. Deciphering Functional Roles of Protein
392 Succinylation and Glutarylation Using Genetic Code Expansion. *Nat. Chem.* **2024**.

393 19. Yang, Y.; Song, H.; He, D.; Zhang, S.; Dai, S.; Lin, S.; Meng, R.; Wang, C.; Chen, P. R. Genetically Encoded
394 Protein Photocrosslinker with a Transferable Mass Spectrometry-Identifiable Label. *Nat. Commun.* **2016**, *7*, 12299.

395 20. Botti, P.; Pallin, T. D.; Tam, J. P. Cyclic Peptides from Linear Unprotected Peptide Precursors through
396 Thiazolidine Formation. *J. Am. Chem. Soc.* **1996**, *118* (42), 10018–10024.

397 21. Wade, J. D.; Domagala, T.; Rothacker, J.; Catimel, B.; Nice, E. Use of Thiazolidine-Mediated Ligation for Site
398 Specific Biotinylation of Mouse EGF for Biosensor Immobilisation. *Letters in Peptide Science* **2001**, *8* (3), 211–220.

399 22. Bi, X.; Pasunooti, K. K.; Tareq, A. H.; Takyi-Williams, J.; Liu, C.-F. Genetic Incorporation of 1,2-Aminothioliol
400 Functionality for Site-Specific Protein Modification via Thiazolidine Formation. *Org. Biomol. Chem.* **2016**, *14* (23),
401 5282–5285.

402 23. Liu, X.; Wang, Y.; Ye, B.; Bi, X. Catalyst-Free Thiazolidine Formation Chemistry Enables the Facile
403 Construction of Peptide/Protein-Cell Conjugates (PCCs) at Physiological pH. *Chem. Sci.* **2023**, *14* (26), 7334–7345.

404 24. Li, K.; Wang, W.; Gao, J. Fast and Stable N-Terminal Cysteine Modification through Thiazolidino Boronate
405 Mediated Acyl Transfer. *Angew. Chem. Int. Ed. Engl.* **2020**, *59* (34), 14246–14250.

406 25. Bi, X.; Yin, J.; Rao, C.; Balamkundu, S.; Banerjee, B.; Zhang, D.; Zhang, D.; Dedon, P. C.; Liu, C.-F.
407 Thiazolidin-5-Imine Formation as a Catalyst-Free Bioorthogonal Reaction for Protein and Live Cell Labeling. *Org.*
408 *Lett.* **2018**, *20* (24), 7790–7793.

409 26. Bandyopadhyay, A.; Cambray, S.; Gao, J. Fast and Selective Labeling of N-Terminal Cysteines at Neutral pH
410 via Thiazolidino Boronate Formation. *Chem. Sci.* **2016**, *7* (7), 4589–4593.

411 27. Faustino, H.; Silva, M. J. S. A.; Veiros, L. F.; Bernardes, G. J. L.; Gois, P. M. P. Iminoboronates Are Efficient
412 Intermediates for Selective, Rapid and Reversible N-Terminal Cysteine Functionalisation. *Chem. Sci.* **2016**, *7* (8),
413 5052–5058.

414 28. Bernardes, G. J. L.; Steiner, M.; Hartmann, I.; Neri, D.; Casi, G. Site-Specific Chemical Modification of
415 Antibody Fragments Using Traceless Cleavable Linkers. *Nat. Protoc.* **2013**, *8* (11), 2079–2089.

416 29. Nakatsu, K.; Okamoto, A.; Hayashi, G.; Murakami, H. Repetitive Thiazolidine Deprotection Using a Thioester-
417 Compatible Aldehyde Scavenger for One-Pot Multiple Peptide Ligation. *Angew. Chem. Int. Ed. Engl.* **2022**, *61* (39),
418 e202206240.

419 30. Jbara, M.; Maity, S. K.; Seenayah, M.; Brik, A. Palladium Mediated Rapid Deprotection of N-Terminal Cysteine
420 under Native Chemical Ligation Conditions for the Efficient Preparation of Synthetically Challenging Proteins. *J.*
421 *Am. Chem. Soc.* **2016**, *138* (15), 5069–5075.

422 31. Jbara, M.; Laps, S.; Morgan, M.; Kamnesky, G.; Mann, G.; Wolberger, C.; Brik, A. Palladium Prompted On-
423 Demand Cysteine Chemistry for the Synthesis of Challenging and Uniquely Modified Proteins. *Nat. Commun.* **2018**,
424 *9* (1), 3154.

425 32. Naruse, N.; Kobayashi, D.; Ohkawachi, K.; Shigenaga, A.; Otaka, A. Copper-Mediated Deprotection of
426 Thiazolidine and Selenazolidine Derivatives Applied to Native Chemical Ligation. *J. Org. Chem.* **2020**, *85* (3),
427 1425–1433.

428 33. Zhao, Z.; Metanis, N. Copper-Mediated Selenazolidine Deprotection Enables One-Pot Chemical Synthesis of
429 Challenging Proteins. *Angew. Chem. Int. Ed. Engl.* **2019**, *58* (41), 14610–14614.

430 34. Nakatsu, K.; Murakami, H.; Hayashi, G.; Okamoto, A. Thiazolidine Deprotection by 2-Aminobenzamide-Based
431 Aldehyde Scavenger for One-Pot Multiple Peptide Ligatio. ChemRxiv. **2021**,

432 35. Mann, G.; Satish, G.; Meledin, R.; Vamisetti, G. B.; Brik, A. Palladium-Mediated Cleavage of Proteins with
433 Thiazolidine-Modified Backbone in Live Cells. *Angew. Chem. Int. Ed. Engl.* **2019**, *58* (38), 13540–13549.

434 36. Casi, G.; Huguenin-Dezot, N.; Zuberbühler, K.; Scheuermann, J.; Neri, D. Site-Specific Traceless Coupling of
435 Potent Cytotoxic Drugs to Recombinant Antibodies for Pharmacodelivery. *J. Am. Chem. Soc.* **2012**, *134* (13), 5887–
436 5892.

437 37. Bi, X.; Pasunooti, K. K.; Lescar, J.; Liu, C.-F. Thiazolidine-Masked α -Oxo Aldehyde Functionality for Peptide
438 and Protein Modification. *Bioconjug. Chem.* **2017**, *28* (2), 325–329.

439 38. Brabham, R. L.; Spears, R. J.; Walton, J.; Tyagi, S.; Lemke, E. A.; Fascione, M. A. Palladium-Unleashed
440 Proteins: Gentle Aldehyde Decaging for Site-Selective Protein Modification. *Chem. Commun. (Camb).* **2018**, *54*
441 (12), 1501–1504.

442 39. Spears, R. J.; Brabham, R. L.; Budhadev, D.; Keenan, T.; McKenna, S.; Walton, J.; Brannigan, J. A.;
443 Brzozowski, A. M.; Wilkinson, A. J.; Plevin, M.; Fascione, M. A. Site-Selective C-C Modification of Proteins at
444 Neutral pH Using Organocatalyst-Mediated Cross Aldol Ligations. *Chem. Sci.* **2018**, *9* (25), 5585–5593.

445 40. Hong, V.; Steinmetz, N. F.; Manchester, M.; Finn, M. G. Labeling Live Cells by Copper-Catalyzed Alkyne-
446 Azide Click Chemistry. *Bioconjug. Chem.* **2010**, *21* (10), 1912–1916.

447 41. Hong, V.; Presolski, S. I.; Ma, C.; Finn, M. G. Analysis and Optimization of Copper-Catalyzed Azide-Alkyne
448 Cycloaddition for Bioconjugation. *Angew. Chem. Int. Ed. Engl.* **2009**, *48* (52), 9879–9883.

449 42. Li, L.; Zhang, Z. Development and Applications of the Copper-Catalyzed Azide-Alkyne Cycloaddition
450 (CuAAC) as a Bioorthogonal Reaction. *Molecules.* **2016**, *21* (10), 1393.

451 43. Muyldermans, S. Nanobodies: Natural Single-Domain Antibodies. *Annu. Rev. Biochem.* **2013**, *82*, 775–797.

452 44. Schumacher, D.; Helma, J.; Schneider, A. F. L.; Leonhardt, H.; Hackenberger, C. P. R. Nanobodies: Chemical
453 Functionalization Strategies and Intracellular Applications. *Angew. Chem. Int. Ed. Engl.* **2018**, *57* (9), 2314–2333.

454 45. Bridge, T.; Wegmann, U.; Crack, J. C.; Orman, K.; Shaikh, S. A.; Farndon, W.; Martins, C.; Saalbach, G.;
455 Sachdeva, A. Site-Specific Encoding of Photoactivity and Photoreactivity into Antibody Fragments. *Nat. Chem. Biol.*
456 **2023**, *19* (6), 740–749.

457 46. Yong, K. W.; Yuen, D.; Chen, M. Z.; Porter, C. J. H.; Johnston, A. P. R. Pointing in the Right Direction:
458 Controlling the Orientation of Proteins on Nanoparticles Improves Targeting Efficiency. *Nano. Lett.* **2019**, *19* (3),
459 1827–1831.

460 47. Pande, J.; Szewczyk, M. M.; Grover, A. K. Phage Display: Concept, Innovations, Applications and Future.
461 *Biotechnol. Adv.* **2010**, *28* (6), 849–858.

462 48. Koerber, J. T.; Thomsen, N. D.; Hannigan, B. T.; Degrado, W. F.; Wells, J. A. Nature-Inspired Design of Motif-
463 Specific Antibody Scaffolds. *Nat. Biotechnol.* **2013**, *31* (10), 916–921.

464 49. Chen, P.-H. C.; Guo, X. S.; Zhang, H. E.; Dubey, G. K.; Geng, Z. Z.; Fierke, C. A.; Xu, S.; Hampton, J. T.; Liu,
465 W. R. Leveraging a Phage-Encoded Noncanonical Amino Acid: A Novel Pathway to Potent and Selective
466 Epigenetic Reader Protein Inhibitors. *ACS. Cent. Sci.* **2024**, *10* (4), 782–792.

467 50. Allen, G. L.; Grahn, A. K.; Kourentzi, K.; Willson, R. C.; Waldrop, S.; Guo, J.; Kay, B. K. Expanding the
468 Chemical Diversity of M13 Bacteriophage. *Front. Microbiol.* **2022**, *13*, 961093.

469 51. Owens, A. E.; Iannuzzelli, J. A.; Gu, Y.; Fasan, R. MORPH-PhD: An Integrated Phage Display Platform for the
470 Discovery of Functional Genetically Encoded Peptide Macrocyces. *ACS. Cent. Sci.* **2020**, *6* (3), 368–381.

471 52. Oller-Salvia, B.; Chin, J. W. Efficient Phage Display with Multiple Distinct Non-Canonical Amino Acids Using
472 Orthogonal Ribosome-Mediated Genetic Code Expansion. *Angew. Chem. Int. Ed. Engl.* **2019**, *58* (32), 10844–10848.

473 53. Tian, F.; Tsao, M.-L.; Schultz, P. G. A Phage Display System with Unnatural Amino Acids. *J. Am. Chem. Soc.*
474 **2004**, *126* (49), 15962–15963.

475 54. Carrico, Z. M.; Farkas, M. E.; Zhou, Y.; Hsiao, S. C.; Marks, J. D.; Chokhawala, H.; Clark, D. S.; Francis, M. B.
476 N-Terminal Labeling of Filamentous Phage to Create Cancer Marker Imaging Agents. *ACS. Nano.* **2012**, *6* (8),
477 6675–6680.

478 55. Wang, R.; Li, H.-D.; Cao, Y.; Wang, Z.-Y.; Yang, T.; Wang, J.-H. M13 Phage: A Versatile Building Block for a
479 Highly Specific Analysis Platform. *Anal. Bioanal. Chem.* **2023**, *415* (18), 3927–3944.

480 56. Ng, S.; Jafari, M. R.; Matochko, W. L.; Derda, R. Quantitative Synthesis of Genetically Encoded Glycopeptide
481 Libraries Displayed on M13 Phage. *ACS. Chem. Biol.* **2012**, *7* (9), 1482–1487.

482 57. Wang, X. S.; Chen, P.-H. C.; Hampton, J. T.; Tharp, J. M.; Reed, C. A.; Das, S. K.; Wang, D.-S.; Hayatshahi, H.
483 S.; Shen, Y.; Liu, J.; Liu, W. R. A Genetically Encoded, Phage-Displayed Cyclic-Peptide Library. *Angew. Chem. Int.*
484 *Ed. Engl.* **2019**, *58* (44), 15904–15909.

485 58. Han, L.; Zhao, Y.; Cui, S.; Liang, B. Redesigning of Microbial Cell Surface and Its Application to Whole-Cell
486 Biocatalysis and Biosensors. *Appl. Biochem. Biotechnol.* **2018**, *185* (2), 396–418.

487 59. Bi, X.; Yin, J.; Nguyen, G. K. T.; Rao, C.; Halim, N. B. A.; Hemu, X.; Tam, J. P.; Liu, C.-F. Enzymatic
488 Engineering of Live Bacterial Cell Surfaces Using Butelase 1. *Angew. Chem. Int. Ed. Engl.* **2017**, *56* (27), 7822–
489 7825.

490 60. Link, A. J.; Vink, M. K. S.; Tirrell, D. A. Presentation and Detection of Azide Functionality in Bacterial Cell
491 Surface Proteins. *J. Am. Chem. Soc.* **2004**, *126* (34), 10598–10602.

492 61. Tuley, A.; Lee, Y.-J.; Wu, B.; Wang, Z. U.; Liu, W. R. A Genetically Encoded Aldehyde for Rapid Protein
493 Labelling. *Chem. Commun. (Camb).* **2014**, *50* (56), 7424–7426.

494 62. Palei, S.; Becher, K. S.; Nienberg, C.; Jose, J.; Mootz, H. D. Bacterial Cell-Surface Display of Semisynthetic
495 Cyclic Peptides. *Chembiochem.* **2019**, *20* (1), 72–77.

496 63. Keeble, A. H.; Turkki, P.; Stokes, S.; Khairil Anuar, I. N. A.; Rahikainen, R.; Hytönen, V. P.; Howarth, M.
497 Approaching Infinite Affinity through Engineering of Peptide-Protein Interaction. *Proc. Natl. Acad. Sci. U. S. A.*
498 **2019**, *116* (52), 26523–26533.

499 64. Rice, J. J.; Daugherty, P. S. Directed Evolution of a Biterminal Bacterial Display Scaffold Enhances the Display
500 of Diverse Peptides. *Protein. Eng. Des. Sel.* **2008**, *21* (7), 435–442.

501 65. Reddington, S. C.; Howarth, M. Secrets of a Covalent Interaction for Biomaterials and Biotechnology: SpyTag
502 and SpyCatcher. *Curr. Opin. Chem. Biol.* **2015**, *29*, 94–99.

- 503 66. Forbes, N. S. Engineering the Perfect (Bacterial) Cancer Therapy. *Nat. Rev. Cancer*. **2010**, *10* (11), 785–794.
- 504 67. Rong, L.; Lei, Q.; Zhang, X.-Z. Engineering Living Bacteria for Cancer Therapy. *ACS. Appl. Bio. Mater.* **2020**,
- 505 3 (12), 8136–8145.
- 506 68. Keeble, A. H.; Howarth, M. Power to the Protein: Enhancing and Combining Activities Using the Spy Toolbox.
- 507 *Chem. Sci.* **2020**, *11* (28), 7281–7291.

508 **Acknowledgements**

509 This study was supported by the National Key Research and Development Program of China
510 (2018YFA0900404), the National Natural Science Foundation of China (22134003), Zhejiang Provincial
511 Natural Science Foundation of China under Grant No. LY24B020008 and Zhejiang University of
512 Technology High-Level Talents Startup Funds (2021414800229, X. B. Bi).

513 **Ethics declarations**

514 Competing interests

515 The authors declare no conflict of interests.